Title page

Modelling the seasonal impacts of a wastewater treatment plant on water quality in a Mediterranean stream using microbial indicators

M. Pascual-Benito[1,2], D. Nadal-Sala[3,4], M. Tobella[3], E. Ballesté[1,2], C. García-Aljaro[1,2], S. Sabaté[3,5], F. Sabater[3,5], E. Martí[6], C. A. Gracia[3,5], A. R. Blanch[1,2], F. Lucena[1,2]

[1]Department of Genetics, Microbiology and Statistics, Faculty of Biology, University of Barcelona, Diagonal 643, 08028, Barcelona, Spain.

[2]The Water Research Institute, University of Barcelona, Montalegre 6, 08001 Barcelona, Spain

[3]Department of Evolutionary Biology, Ecology and Environmental Sciences, University of Barcelona, Diagonal 643, 08028, Barcelona, Spain.

[4]IMK-IFU (Karlsruhe Institute of Meteorology and Climate Research-Atmospheric Environmental Research), Kreuzeckbahnstraße 19, 82467 Garmisch-Partenkirchen, Germany.

[5]CREAF (Center for Ecological Research and Forestry Applications), 08193, Cerdanyola del Vallès, Spain.

[6]Integrative Freshwater Ecology Group, Centre for Advanced Studies of Blanes (CEAB-CSIC), 17300, Blanes, Spain

[*]To whom correspondence should be addressed. Miriam Pascual-Benito: Tel: +349340309044; Fax: +34934039047. mpascualbenito@ub.edu

Keywords: faecal pollution, microbial indicators, environmental drivers, microbial inactivation, Microbial Source Tracking, self-depuration distance

HIGHLIGHTS

- Decay rates of five faecal indicator organisms in a Mediterranean stream affected by a wastewater treatment plant are reported.
- Air temperature and streamflow are the main drivers of indicator behaviour.
- Decay rates of microbial indicators have been modelled seasonally.
- The impact of a WWTP has been modelled in terms of stream self-depuration.
- The self-depuration distance metric could be a useful tool in water management strategies.

Modelling the seasonal impacts of a wastewater treatment plant on water quality in a Mediterranean stream using microbial indicators

M. Pascual-Benito[1,2], D. Nadal-Sala[3,4], M. Tobella[3], E. Ballesté[1,2], C. García-Aljaro[1,2], S. Sabaté[3,5], F. Sabater[3,5], E. Martí[6], C. A. Gracia[3,5], A. R. Blanch[1,2], F. Lucena[1,2]

[1]Department of Genetics, Microbiology and Statistics, Faculty of Biology, University of Barcelona, Diagonal 643, 08028, Barcelona, Spain.

[2]The Water Research Institute, University of Barcelona, Montalegre 6, 08001 Barcelona, Spain.

[3]Department of Evolutionary Biology, Ecology and Environmental Sciences, University of Barcelona, Diagonal 643, 08028, Barcelona, Spain.

[4]IMK-IFU (Karlsruhe Institute of Meteorology and Climate Research-Atmospheric Environmental Research), Kreuzeckbahnstraße 19, 82467 Garmisch-Partenkirchen, Germany.

[5]CREAF (Center for Ecological Research and Forestry Applications), 08193, Cerdanyola del Vallès, Spain.

[6]Integrative Freshwater Ecology Group, Centre for Advanced Studies of Blanes (CEAB-CSIC), 17300, Blanes, Spain.

[*]To whom correspondence should be addressed. Miriam Pascual-Benito: Tel: +349340309044; Fax: +34934039047. mpascualbenito@ub.edu

Keywords: faecal pollution, microbial indicators, environmental drivers, microbial inactivation, Microbial Source Tracking, self-depuration distance

ABSTRACT

Faecal pollution modelling is a valuable tool to evaluate and improve water management strategies, especially in a context of water scarcity. The reduction dynamics of five faecal indicator organisms (*E. coli*, spores of sulphite-reducing clostridia, somatic coliphages, GA17 bacteriophages and a human-specific *Bifidobacterium* molecular marker) were assessed in an intermittent Mediterranean stream affected by a wastewater treatment plant (WWTP). Using Bayesian inverse modelling, the decay rates of each indicator were correlated with two environmental drivers (temperature and streamflow downstream of the WWTP) and the generated model was used to evaluate the self-depuration distance (SDD) of the stream. A consistent increase of 1-2 $\log_{10}$ in the concentration of all indicators was detected after the discharge of the WWTP effluent. The decay rates showed seasonal variation, reaching a maximum in the dry season, when SDDs were also shorter and the stream had a higher capacity to self-depurate. High seasonality was observed for all faecal indicators except for the spores of sulphite-reducing clostridia. The maximum SDD ranged from 3 km for the spores of sulphite-reducing clostridia during the dry season and 15 km for the human-specific *Bifidobacterium* molecular marker during the wet season. The SDD provides a single standardized metric that integrates and compares different contamination indicators. It could be extended to other Mediterranean drainage basins and has the potential to integrate changes in land use and catchment water balance, a feature that will be especially useful in the transient climate conditions expected in the coming years.

1. INTRODUCTION

Water scarcity is currently threatening many areas of the planet, with severe implications both for ecosystems and the well-being of human societies. One such area is the Mediterranean basin, where already 80 million people are living below the water poverty threshold of 500 $m^3 \cdot person^{-1} \cdot year^{-1}$ (Milano et al., 2013), and ca. 60% of the renewable freshwater resources are currently being used by the population (Thivet and Blinda, 2011).

The Mediterranean climate is characterized by a strong seasonality in precipitation, with most of it concentrated in early spring and late autumn (Lionello et al., 2006). Recurrent summer drought stress drastically reduces the flow of Mediterranean rivers (Otero et al., 2011; Bonada and Resh, 2013). Moreover, climate projections for the 21st century predict a sharp increase in global temperature, a 10 to 15% decrease in precipitation in the Mediterranean by the year 2050, a concentration of precipitation in fewer but more intense events, and an increase in rain seasonality, thus reducing not only summer but also winter and spring precipitation (Lionello et al., 2014; Lionello and Scarascia, 2018). The higher temperatures will also reduce water availability due to higher levels of evapotranspiration (IPCC, 2013; Mariotti et al., 2015; Serrano-Notivoli et al., 2018). Under such circumstances, a reduction in streamflow during summer is expected, as well as longer zero-flow periods. In addition, anthropogenic pressure, understood as an increase in water demand and faecal pollution discharge into rivers, is predicted to increase in Mediterranean ecosystems in the next decades, thus amplifying the impacts of climate change (Bonada and Resh, 2013; IPCC, 2013; Stella et al., 2013).

Wastewater treatment plants (WWTP) are designed to reduce pollutant concentration and to avoid the direct discharge of wastewater into rivers. However, their effluents are still an important source of pollutants and faecal microorganisms, including pathogens. In the Mediterranean summer, reductions in water flow lead to higher concentrations of these pollutants (Merseburger et al., 2005; Mosley, 2015), and WWTP effluents may constitute most of the flow in intermittent streams (Muñoz et al., 2009). Extreme rainfall events are also associated with a higher concentration of waterborne pathogens, caused by the re-mobilization of river sediments to which they are attached (García-Aljaro et al., 2017; Jamieson et al., 2005; Martín-Díaz et al., 2017). Intense precipitation may also lead to an oversaturation and disruption of WWTP functionality (Curriero et al., 2001), as well as a reduction of the decay rates of faecal microorganisms due to decreased river bio-reactivity (Jonsson and Agerberg, 2015; Merseburger et al, 2005). Increases in pollutant concentrations may result in human health risks due to pathogen exposure (Auld et al., 2004; Curriero et al., 2001; Rose et al., 2010; Super et al., 1981), thereby compromising water usability (WHO, 2017).

Faecal microorganisms, including pathogens, are released by WWTP effluents into rivers and subjected to inactivation while being transported downstream (Agulló-Barceló et al., 2013; Jonsson and Agerberg, 2015). The assessment of the entire range of pathogen microorganisms would be difficult and expensive, so microbial indicators are frequently used in water quality management (García-Aljaro et al., 2018; Saxena et al., 2015; WHO, 2009, 2001). However, each microbial indicator may respond differently to exogenous factors such as water temperature, solar irradiance, dilution, predation, sedimentation or re-suspension (Auer and Niehaus, 1993; Ballesté et al., 2018; Martín-Díaz et al., 2017). Self-depuration distance (SDD) is proposed here as a standardized metric (in km) integrating all available indicator information to assess the distance needed to recover water quality downstream of the WWTP.

Five faecal indicator organisms (FIO) were selected and their in-stream decay rates were monitored downstream of the WWTP. The SDD, defined as the distance needed to return to the indicator concentrations upstream of the WWTP, was assessed as a measure to provide information about the spread of faecal pollution in water. Previous studies of FIOs in rivers have focused on inactivation time rather than distance (Dankovich et al., 2016; Fiorentino et al., 2018; Jonsson and Agerberg, 2015; Muirhead et al., 2004; Vinten et al., 2004). However, the pollutant travel distance per unit of time for a given river is dependent on river discharge (Runkel, 1998). The purpose of the SDD metric is to evaluate how far downstream the WWTP may negatively impact the water quality, taking into account the impact of seasonal variations on river discharge. This impact is implicit in the metric, rather than being added *a posteriori*, as it is based on inactivation distance rather than inactivation time.

The aims of this research were to: i) study and compare the seasonal dynamics of different faecal indicator organisms in a low-order Mediterranean stream affected by a WWTP effluent; ii) assess the SDD considering seasonal variations; iii) model in-stream pollutant SDD dynamics according to different environmental drivers, and iv) use the SDD metric to integrate and compare modelled pollutant dynamics.

The initial hypotheses of the study were: i) the inactivation of microbial indicators, and consequently the SDD, presents a seasonal behaviour, assuming that ii) the main factors explaining the SDD are streamflow and temperature (Ballesté and Blanch, 2010; Burkhardt et al., 2000; García-Aljaro et al., 2018), and iii) the decay rates of most conservative microbial indicators are less dependent on environmental conditions (Martín-Díaz et al., 2017).

2. MATERIAL AND METHODS

2.1 Study site

The *Riera de Cànoves* is a third-order stream ca. 50 km north-east from Barcelona (NE Spain). Its source is located in the Natural Park and Biosphere Reserve of the Montseny mountain range and it has a catchment of 16.4 km^2 until the Cànoves-Samalús WWTP. The catchment is dominated by a siliceous substrate of granite and schist and it has smooth slopes (2%) (Catalan Cartographic Institute, 2018). Forest cover of the catchment is 77% and land uses include irrigated agriculture of cereals and legumes (15%) and a small cattle ranching industry (~0.1%). Although the urbanized fraction of the area is small (~5%), it is disseminated throughout the catchment in residential zones, thus implying concomitant basal human pollution. Climate characteristics correspond to sub-humid Mediterranean, with mild winters, wet springs, and dry summers. In the 1996-2017 period, the mean annual temperature averaged 12.0°C (Catalan Meteorological Service) and the annual precipitation averaged 780.8 mm, with values ranging from 600 to 1000 mm·year^{-1}. Located in the first 4 km of the stream, the

Vallforners reservoir, with a 2.1 hm^3 maximum storage capacity and a consistent output flow of about 0.005 $m^3 \cdot s^{-1}$ throughout the year, strongly regulates the streamflow dynamics downstream. As a result of water demand, evapotranspiration and lack of rainfall, waterflow between the reservoir and the WWTP is sometimes zero.

The WWTP of *Cànoves-Samalús* treats the water of 9,200 inhabitant-equivalents. The plant consists of a pre-treatment and biological treatment system using activated sludge, with a complete mixture and two concentric reactor-decanter lines. Daily discharge of the WWTP ranges from 0.008 to 0.02 $m^3 \cdot s^{-1}$, with slightly higher values in spring and winter than in summer and autumn (Figure 1). The riverbed downstream of the WWTP is a mixture of rock and stones (5%), gravel (40%), sand (40%) and silt and clay (15%).

Twelve sampling campaigns were performed during 2016-2017. Water samples were collected at 9 different points of the *Riera de Cànoves*: i) a site located 150 meters upstream of the WWTP, ii) the WWTP effluent, iii) a 450 m-long stretch downstream of the WWTP where 6 samples were collected every 75 m (75 m, 150 m, 225 m, 275 m, 350 m and 450 m downstream of the WWTP) and iv) a point located 1000 m downstream of the WWTP. Water samples were collected from the surface of the stream in sterile containers and transported to the laboratory at 4°C. Analyses were performed within 8 hours of collection.

2.2 Microbial detection and enumeration

Culturable *Escherichia coli* and spores of sulphite-reducing clostridia (SSRC) were selected as bacterial indicators, as they show different behaviour: *E. coli* is a non-conservative microbial indicator mostly used to detect faecal pollution, whereas the highly resistant SSRC is a conservative indicator that proxies the presence of protozoa oocysts and helminth ova (Agulló-Barceló et al., 2013).

Culturable *E. coli* were enumerated using a pour plate method in Chromocult® agar (Merck, Darmstadt, Germany). Dark blue and/or purple colonies were counted after an overnight incubation at 44˚C (Astals et al., 2012).

To enumerate SSRC, samples were subjected to a thermal shock at 80˚C for 10 minutes, anaerobically cultured by mass inoculation in *Clostridium perfringens* selective agar (Scharlab, Barcelona, Spain) and incubated overnight at 44˚C, as previously described (Ruiz-Hernando et al., 2014).

Two bacteriophages were used as viral indicators: somatic coliphages (SOMCPH), related to general faecal pollution, and bacteriophages infecting *Bacteroides thetaiotaomicron* strain GA17 (GA17PH), associated with human pollution and used as microbial source tracking (MST) markers to determine the origin of pollution in water (Jofre et al., 2014). SOMCPH and GA17PH were enumerated by the double agar layer technique as indicated in the ISO standards 10705-2 and 10705-4 (ISO, 2001, 2000), respectively. In order to detect human-specific bacteriophages, the ISO standard 10705-4 was modified by using *Bacteroides thetaiotaomicron* strain GA17 (Muniesa et al., 2012).

A molecular marker targeting human-specific *Bifidobacterium* (HMBif) was also analysed by qPCR as in previous studies (Gómez-Doñate et al., 2012). For this, DNA was extracted from different sample volumes (from 0.2 to 0.5 l) according to the amount of suspended particles able to saturate the membranes. Samples were concentrated by filtration through a polycarbonate membrane with a pore size of 0.22 µm (SO-PAK, Millipore, Darmstadt, Germany). Membranes were then placed in 0.5 ml of GITC buffer (5 M guanidine thiocyanate, 100 mM EDTA [pH 8.0], 0.5% sarkosyl) and frozen at -20°C in lysis buffer until DNA extraction. The DNA was extracted using the QIAamp DNA Blood Mini Kit (Qiagen GmbH, Hilden, Germany) with some modifications (Gourmelon et al., 2007). Samples, negative controls, DNA extraction controls and five points on the standard curve were analysed for two replicates by qPCR, as previously described (Gómez-Doñate et al., 2012).

2.3 Streamflow calculation

In order to calculate the streamflow above the WWTP, twelve additions of NaCl, a conservative tracer, were performed (Gordon et al., 1992). Briefly, this method estimates the streamflow from a known concentration of a conservative tracer, whose signal records in-stream conductivity. In each addition, 1 l of solution of known conductivity was added to the stream, and the streamflow was estimated by the integration of the in-stream conductivity breakthrough curve corrected by basal conductivity. To obtain the conservative-tracer breakthrough curves, electrical conductivity (EC, $\mu S \cdot cm^{-1}$) was measured with a portable conductivity meter (WTW, Weilheim, Germany) at the bottom of the reach every 5 seconds during the solute injection.

Additionally, one piezometer was placed in the riverbank 150 m upstream of the WWTP at a depth of 50 cm. A pressure sensor (HOBO® U20-001-04 Water Level Logger) was placed inside the piezometer to record changes in pressure corresponding to changes in streamflow. In order to differentiate between pressure changes due to increases in water level and atmospheric pressure, another sensor was placed near the stream but outside the water. A continuous daily discharge time-series was obtained by non-linear regression between the daily averaged water level record against the twelve discrete streamflow measurements by conservative tracer addition. Gaps in the atmospheric pressure register were filled with observations from a nearby meteorological station.

Daily effluent discharge ($Q_{effluent}$) values were obtained from the WWTP register during the same period. During heavy rainfall or maintenance operations, the WWTP allowed a bypass of non-treated water, thus exponentially increasing its discharge into the stream. The $Q_{effluent}$ time-series has been corrected to avoid these anomalous flow peaks by assuming a $Q_{effluent}$ equal to the monthly median $Q_{effluent}$ when $Q_{effluent}$ was higher than 95% monthly values or lower than 5% monthly values. This correction was applied to 21 registers, which corresponded to less than 3% of the daily values. No seasonal trend was observed.

The streamflow was classified to study its seasonality. The dry season was defined as the period when the streamflow upstream of the WWTP was lower than 0.005 $m^3 \cdot s^{-1}$ and the dilution factor was lower than 0.1, which corresponded to summer. The wet season was the period when the streamflow was higher than 0.005 $m^3 \cdot s^{-1}$ and the dilution factor was higher than 0.1, which corresponded to the other seasons (Figure 1d).

Meteorological data (i.e. daily mean air temperature and atmospheric pressure) was supplied by MeteoCat (Catalan Meteorological Service) from Tagamanent meteorological station, located ca. 9.5 km northwest of the WWTP.

2.4 Data analysis and modelling approach

2.4.1 Data analysis

A two-sample T-test was performed to analyse seasonal differences for each FIO concentration before and after the WWTP. Normality of log-transformed FIO concentrations was confirmed by a Shapiro-Wilk test.

2.4.2 Measured self-depuration distance

The concentration of each individual indicator was obtained after the WWTP effluent (I_0) for each sampling campaign [in (log(cfu·l^{-1}), log(pfu·l^{-1}) or log(GC·l^{-1})].

Eq.1] $$I_0 = \frac{I_{stream} \cdot Q_{stream} + I_{effluent} \cdot Q_{effluent}}{Q_{stream} + Q_{effluent}}$$

where I_{stream} is the indicator concentration in the stream before the WWTP effluent [(log(cfu·l^{-1}), log(pfu·l^{-1}) or log(GC·l^{-1})], Q_{stream} is the flow upstream of the WWTP effluent (m^3·s^{-1}), $I_{effluent}$ is the indicator concentration in the WWTP effluent [(log(cfu·l^{-1}), log(pfu·l^{-1}) or log(GC·l^{-1})] and $Q_{efflluent}$ is the discharge of the WWTP effluent (m^3·s^{-1}).

For each sampling campaign and studied indicator, the natural logarithm of the concentration obtained at sampling points downstream of the WWTP was related to the distance to the WWTP effluent by a linear least squares approach, the decay rate (*k*, in km^{-1}) thus being the negative slope of the linear relationship between the concentration of a given indicator and the distance.

Each indicator concentration at d distance after the WWTP effluent (I_d) was modelled by an exponential decay rate depending on an indicator-specific decay rate (*k*) and the distance to I_0, according to the logarithm form of Chick's equation (Chick, 1908)

Eq.2] $$I_d = I_0 e^{(-kd)}$$

where I_d is the indicator concentration [(log(cfu·l^{-1}), log(pfu·l^{-1}) or log(GC·l^{-1})] at a given distance (d) from the WWTP effluent (d, in km) and *k* the decay rate, which varies between each sampling campaign and indicator.

From "*in situ*" I_{stream}, I_0, and *k* measurements, and assuming no changes in streamflow downstream of the WWTP, equation 2 was re-arranged in order to calculate the SDD (in km) for each microbial indicator.

Eq.3] $$SDD = \frac{\ln(I_{stream}) - \ln(I_0)}{k}$$

2.4.3 Modelling *k* from streamflow and temperature

In order to model how changes in temperature and streamflow affected the SDD, the relationship of the *k* coefficient with measured streamflow and air temperature was modelled for each sampling campaign according to

Eq.4] $$k_i = f(T_i) + f(D_i) + \varepsilon_i$$

where k_i is the decay rate (*k*) for a given FIO and campaign, T_i is the mean daily air temperature during the *i* campaign, D_i is the mean daily flow during the *i* campaign and ε_i is the error. Air temperature was used instead of water temperature due to the reliability of the meteorological data and the fact that air temperature and water temperature are highly correlated in low-discharge rivers on a daily basis (Morrill et al., 2005; Pilgrim et al., 1998). Thus, it was assumed that *k* responses to air temperature were reproducing *k* responses to water temperature.

Theoretically, it was expected that a higher temperature would accelerate the decay rate due to enhanced biological, physical and chemical processes, while an increasing streamflow would reduce it (Jonsson and Agerberg, 2015). Thus, equation 5 dependencies on temperature and streamflow may be expressed as:

Eq.5] $$f(T_i) = \frac{a}{b + \exp^{(-\mathrm{T_i} * \mathrm{c})}}$$

Eq.6] $$f(Q_{downstream}) = d * Q_{downstream}{}^{e}$$

where *a, b, c, d* and *e* are empirically determined unitless coefficients, T_i is the daily mean temperature in °C, and $Q_{downstream}$ is the mean daily streamflow after WWTP discharge (i.e. $Q_{downstream} = Q_{stream} + Q_{effluent}$).

A likelihood-based inverse Bayesian model calibration (Hartig et al., 2012) was used. This robust approach has proved to be a very useful tool when data is scarce, or when using models with a high number of parameters (Hartig et al., 2014; Lagarrigues et al., 2015; O'Hara et al., 2002; Purves et al., 2007). However, as complete Bayesian calibration may be computationally expensive, only the set of parameters providing the optimal fit of the model to observations was considered (i.e. a maximum *"a posteriori"* estimation approach). A double-exponential (Laplace) error function was selected, as it makes the likelihood function less sensitive to outliers compared to the Gaussian error distribution function (Augustynczik et al., 2017). Bayesian approaches were also needed for prior parameter distributions. A flat, wide, non-informative uniform prior distribution for all parameters was assumed with boundaries determined by expert judgment. After building the likelihood function and establishing the prior distribution, Bayesian optimizations were run using the "DEOptim" R package (Ardia et al., 2011; Mullen et al., 2011), which performs a Bayesian parameter optimization using a Differential-Evolution MCMC with a memory and snooker update sampler (Ter Braak and Vrugt, 2008).

2.4.4 Obtaining monthly k_i and SDD

Daily k_i values were calculated from equations 4, 5 and 6 with the empirical coefficients obtained for each FIO and daily observed Q and T. Then, I_0 was calculated daily following equation 1, and according to daily measured Q_{stream} and $Q_{effluent}$. As no significant seasonal trend in I_{stream} and $I_{effluent}$ was observed throughout the experiment, the uncertainty of SDD related to unknown FIO concentrations was evaluated as follows: for each FIO and for I_{stream} and $I_{effluent}$, mean ± SD were obtained, as well as their 95% CI. Then, the sensitivity of model outputs to I_{stream} and $I_{effluent}$ was assessed by obtaining 1,000 random samples of daily I_{stream} and $I_{effluent}$ for each FIO, according to a truncated normal N ($\bar{x}$=mean, σ^2=sd, min =5%CI, max=95%CI). No temporal autocorrelation was accounted for in daily random sample generation. For a given I_0, I_{stream} and $k_{i,}$ the daily SDD was calculated for the 2016-2017 period according to equation 3. Finally, SDD values were integrated as median daily ± 95% CI values from the 1,000 random samples. Daily k_i and SDD values were reported as median monthly values (± 95CI in the case of SDD to account for I_{stream} and $I_{effluent}$ uncertainty in model projections), to make the results more easily understandable.

3. RESULTS AND DISCUSSION

3.1 Observed flow data

Even considering the constant output from the Vallforners reservoir, the flow of the *Riera de Cànoves* was strongly seasonal above the WWTP due to fluctuating precipitation, evapotranspiration and water extraction for agricultural purposes. The flow data upstream of the WWTP obtained during 2016-2017 ranged from 0 $m^3 \cdot s^{-1}$ to 0.015$m^3 \cdot s^{-1}$, with dry season values of zero or close to zero. WWTP contributions to streamflow were also slightly seasonal, with values ranging from 0.015 $m^3 \cdot s^{-1}$ during the wet season to 0.007 $m^3 \cdot s^{-1}$ during the dry season. Downstream of the WWTP, streamflow ranged from about 0.007 $m^3 \cdot s^{-1}$ during the summer to an observed peak of 0.03 $m^3 \cdot s^{-1}$ in the spring of 2017 (Figure 1). The dilution factor ranged from 0 in the dry season to 0.5 in the wet season, thus reflecting the high impact of WWTP water input on the *Riera de Cànoves*. Continuous Q records were used to calculate *k* and SDD for the different FIOs as a model input.

3.2 Seasonal faecal indicator dynamics.

A basal faecal pollution was consistently and repeatedly detected above the WWTP due to human-origin diffuse pollution from isolated houses with septic systems, and the presence of wildlife and farming activities in the surrounding area. The concentrations observed were in accordance with reports for similar streams (Ishii and Sadowsky, 2008; Nguyen et al., 2018) (Table 1). Nonetheless, a statistically significant increase of 1-2 $\log_{10}$ was observed in the concentration of each FIO downstream of the WWTP compared to the values obtained upstream

($p<0.05$), indicating that the WWTP effluent constituted an input of faecal pollution into the stream. No statistically significant differences were found in seasonal FIO concentrations downstream of the WWTP, with within-season variability higher than between-season, which suggested that most of the FIOs belonged to the WWTP effluent (Table 1). Moreover, no differences in FIO concentrations were observed below the WWTP, even considering that during the wet season Q_{stream} provided ca. 45-50% of the downstream streamflow, while during the dry season $Q_{downstream}$ consisted almost entirely of $Q_{effluent}$, indicating that dilution was not a crucial factor.

A gradual reduction in concentration was observed for all the studied FIOs downstream of the WWTP, with indicator-specific decay rates (Table 2). Irrespective of season, the decay rates were higher for *E coli*, the non-conservative indicator, than for SSRC, the conservative indicator, whereas the viral and MST markers, as semi-conservative indicators, presented intermediate values. Additionally, decay rates for all FIOs presented seasonal differences, being higher in the dry season, though statistically significant differences were only observed for SOMCPH ($p<0.05$).

Also showing seasonality, the measured SDDs for all target FIOs were higher in the wet than the dry season (Table 2). Nevertheless, those differences were only statistically significant for *E. coli* ($p<0.01$), which presented an SDD of 0.6 km during the dry season and 3.1 km during the wet season. In this study, the dry season, when the flow upstream of the WWTP was nearly 0 $m^3 \cdot s^{-1}$, coincided with the highest temperatures. These results are in agreement with previous studies (Ballesté et al., 2018; Ballesté and Blanch, 2010; Bonjoch et al., 2009; Fauvel et al., 2017; Wu et al., 2016) where the seasonality of decay rates for different FIOs was strongly correlated to changes in temperature. Concurrently, SDDs were related with decay rates, indicating that in the wet season the stream capacity to self-depurate decreased, as longer transport distances were needed to return to the concentrations upstream of the WWTP. In contrast, in the dry season, increased evapotranspiration due to higher temperatures and lower precipitation reduced the streamflow, increasing the water residence time and therefore the decay rates. The higher decay rates may be due to enhanced in-stream biotic processes such as predation (Romo et al., 2013), but also to abiotic processes such as increased sedimentation (Yakirevich et al., 2013) or longer exposure to sunlight (Sinton et al., 2002)

3.3 Modelling environmental drivers for faecal indicator organisms

After calibration, the statistical model successfully captured the effect of environmental drivers [i.e. daily mean air temperature (T, in °C) and daily mean flow after the WWTP effluent ($Q_{downstream}$, in $m^3 \cdot s^{-1}$)] upon *k* coefficients (Figure 2, Supplementary material 1). Regarding the FIOs, the R^2 between the observed and modelled *k* ranged from 0.6 for SSRC to 0.96 for GA17PH, with a root mean square error (RMSE) ranging from $7 \cdot 10^{-4}$ in *E. coli* to $1 \cdot 10^{-4}$ in SSRC. Among the bacterial indicators, *E. coli* presented the best model fit (R^2 = 0.77, RMSE= $7 \cdot 10^{-4}$) to measured *k*, whilst SSRC presented the worst (R^2 = 0.6, RMSE = $1 \cdot 10^{-4}$). On the other hand, the model reproduced well the observed *k* values for the viral and MST indicators, with R^2 scores of 0.85-0.96, and RMSE values of roughly $2 \cdot 10^{-4}$ for each of the three FIOs. The poorer predictive capacity for SSRC may be attributable to the low correlation between SSRC decay rates and environmental factors. Some authors have reported that SSRC decay rates are less related to climate than to other aspects not taken into account in the current study, such as predation, sedimentation and resuspension (Galfi et al., 2016; García-Aljaro et al., 2017). Moreover, previous studies have reported similar responses of non-conservative *E. coli* and semi-conservative viral and MST indicators to environmental factors (Ahmed et al., 2014; Bonjoch et al., 2009; Davies et al., 1995; Jonsson and Agerberg, 2015; Sinton et al., 2002), with temperature and solar irradiance being the most important parameters explaining their behaviour. Other environmental determinants (e.g. oxygen, redox potential and particle re-suspension) were indirectly taken into account in our study, due to their correlation with the seasonality of the streamflow (Capello et al., 2016). Solar radiation, which can play an important role in bacterial inactivation (Sinton et al., 2002), was implicitly included in air temperature changes, as it is difficult to discriminate between the effect of these two highly correlated parameters (Spearman's r=0.75) (Hassan et al., 2016; Li et al., 2014; Prieto et al., 2009).

All FIOs responded similarly to the two environmental drivers considered, with maximum decay rates at higher temperatures and lower streamflow. Conversely, the decay rates were lower during conditions of low flow and lower temperatures (Figure 3). All FIOs responded similarly to changes in flow, except for SSRC, which were practically unaffected by flow increases (Figure 3a). This trend could be explained by the higher velocity of a stronger streamflow, which implies a shorter water residence time. No dilution effect on inactivation constants was observed, suggesting it is negligible compared to other factors, including those accounted for in the model, i.e. total river discharge and temperature.

FIO decay rates differed in response to temperature increments (Figure 3b); for instance, *E. coli* and GA17PH were more affected by environmental factors and temperature increases compared to SOMCPH and HMBif. These results confirm the non-conservative behaviour of *E. coli* (Bonjoch et al., 2009; Davies et al., 1995), and the semi-conservative behaviour of SOMCPH and HMBif (Ballesté et al., 2018; García-Aljaro et al., 2018; Sinton et al., 1999). Although SSRC are resistant and conservative indicators (Agulló-Barceló et al., 2013; Galfi et al., 2016; Pascual-Benito et al., 2015), they may have been affected by the stimulatory effect of high temperatures on biological processes such as predation (Beveridge et al., 2018). The low concentrations of the semi-conservative viral indicator GA17PH could also explain its strong response to temperature increases.

Finally, to shed light on the contribution of temperature and streamflow to the decay rates, the fraction of the total decay rate caused by temperature was calculated for the whole study period (Figure 4). The contribution of temperature was strongly seasonal, increasing in autumn, peaking in winter and decreasing in spring to reach the lowest values in the summer months. This trend was repeated for each FIO, albeit with some differences. The SSRC decay rate could be explained by temperature throughout the period, the contribution ranging from 80% in summer to 100% in autumn. In contrast, the contribution of temperature to the HMBif decay rate ranged from 5% in summer to 40% in winter; and for *E. coli*, SOMCPH and GA17PH decay rates showed similar variations, the contribution ranging between 20% in summer and 90% in winter. Although the highest contributions of temperature to the total decay rates were expected in summer, the results showed otherwise. This may be explained by the very low summer streamflow, which increased water residence time and led to streamflow replacing temperature as the most important factor in the decay rate.

3.4 Modelling seasonal *k* and SDD for faecal indicator organisms

The decay rates of the studied FIOs were modelled for the 2016-2017 period with environmental data (i.e. T and Q) (Figure 5). Seasonal variations in modelled *k* were observed for all FIOs and the general trend was an increase of *k* from May to September followed by a sharp decline in autumn and winter in both years. Those variations were more or less robust depending on the indicator behaviour. However, very low seasonal variations in SSRC *k* were observed, which indicates a high decoupling of the decay rates from environmental drivers. This is in accordance with what is expected from a resistant microbe and confirms its conservative indicator behaviour. SSRC are therefore of great value for assessing the impact of a WWTP in rivers using SDD measurements.

The modelled SDD also showed quite pronounced seasonal variations according to the studied FIO (Figure 6). The highest SDD was found for HMBif in the winter of 2017, when ca. 15 km were required to decrease its concentration to the levels observed upstream of the WWTP. When all FIOs were considered together, the minimum modelled distance needed for the stream to self-depurate was just under 3 km; SSRC and HMBif had the most impact during the dry season, whereas the maximum SSD was found in winter, driven by HMBif. However, the strong seasonal changes may be attributable to the particularly high concentrations of HMBif upstream of the WWTP, and the fact that it is detected in both active and inactive forms. Regarding SSRC, constant SDD values reflect that these indicators were practically unaffected by environmental conditions. It should be noted that the minimum modelled SDDs were lower than 1 km for *E. coli* and GA17PH in August, when WWTP dilution was null, indicating the stream had a high capacity for self-depuration.

A combined maximum SDD could be particularly useful for water management practices, since it would allow a distance threshold to be established, below which river water would be considered unsuitable for human use due to the health risks associated with WWTP water pouring. During the wet season, the combined SDD was 5-fold higher than during the dry season. This extremely marked seasonal behaviour indicates the need for season-specific water management practices, especially in summer, when water availability in the Mediterranean area is expected to fall in the future (Cook et al., 2014; Orlowsky and Seneviratne, 2013).

Many models have been developed to describe the origin, transport, fate and processes related to faecal microbial pollution as well as to predict the faecal microbial load in catchments, using different tools and techniques such as Geographic Information Systems and simulations (Cho et al., 2016). Moreover, inactivation distances have been used previously by researchers to provide valuable information for water management (Fauvel et al., 2017; Jonsson and Agerberg, 2015). The model presented here, based on multiple FIOs and their environmental drivers, which are easy to measure in the field, constitutes a new tool to determine the spread of faecal pollution and predict the impact of a WWTP on water quality. Furthermore, the SDD provides a metric capable of integrating all types of water quality indicators when assessing WWTP impacts, not only FIOs but also ecological and chemical factors. Thus, the developed model could provide cross-cutting knowledge for water management that may be crucial in the coming years. Climate change, leading to higher temperatures and lower streamflow, is expected to reduce the SDD for all FIOs. However, land use changes together with growing human pressure may increase $Q_{effluent}$ and FIO load, thus increasing faecal microbial concentration downstream of the WWTP. Under such circumstances, non-linear responses of SDD should be expected, as SDD is dependent on *k*, but also sensitive to FIO concentration (Figure 6). Likewise, the clear relationship found between the SDD for FIOs and easily measurable environmental drivers opens an interesting field of research focused on anticipating how global change will affect water quality in the near future, and how in-stream self-depuration processes will interact with ever-increasing human pressure.

Further research should be directed to obtaining a broader range of "*in-situ*" decay rate estimates in order to increase the predicative power of the model, as well as to include in the “k” coefficient other processes found to affect FIO inactivation rates, such as sedimentation, sediment resuspension or predation. Adding them to the model might help to differentiate their effect from that of temperature and streamflow, although the inclusion of highly correlated covariates has been observed to hinder model performance (Andrade et al., 1999; Zhao and Yu, 2006). Finally, implementing the model in other contrasting catchments is essential to test its strengths. If the SDD metric demonstrates its robustness when applied to other study cases under different climate conditions, it might become a crucial tool for assessing WWTP impacts on water quality in future climate conditions, and therefore for evaluating the optimum water management practices in a drier and warmer Mediterranean region.

CONCLUSIONS

- The WWTP effluent significantly increased the concentration of all faecal microbial indicators downstream of the WWTP. While being transported downstream, the FIOs were reduced to a greater or lesser degree according to their inherent characteristics and the environmental drivers, although no seasonality was observed in their concentrations.
- The lowest SDDs were observed during the dry season, indicating this is when the capacity of the stream to recover from the WWTP impact is highest.
- Temperature and streamflow successfully explained decay rates and SDDs. Temperature contribution was minimal in summer, when the contribution of a low flow was more relevant.
- Seasonal differences in the SDD of a range of FIOs were captured by the developed SDD metric. This approach allows different faecal pollutants to be integrated in a single standardized metric.

- If validated in other Mediterranean water courses, the SSD metric has the potential to help water managers to anticipate the effects of climate change on water quality depending on a few environmental drivers, thus improving their ability to adapt to future climate conditions.

ACKNOWLEDGEMENTS

This work was supported by Spanish Ministerio de Economía y Competitividad MEDSOUL project (CGL2014-59977-C3-1-R) and the Catalan government (2017 SGR 170). M. P-B and D. N-S are supported by a FPI grant of the Spanish Ministerio de Economía y Competitividad (BES-2015-072112 and BES-2015-072983 respectively).

CONFLICT OF INTEREST

The authors declare no conflict of interest.

REFERENCES

Agulló-Barceló, M., Oliva, F., Lucena, F., 2013. Alternative indicators for monitoring Cryptosporidium oocysts in reclaimed water. Environ. Sci. Pollut. Res. 20, 4448–4454. https://doi.org/10.1007/s11356-012-1400-4

Ahmed, W., Gyawali, P., Sidhu, J.P.S., Toze, S., 2014. Relative inactivation of faecal indicator bacteria and sewage markers in freshwater and seawater microcosms. Lett. Appl. Microbiol. 59, 348–354. https://doi.org/10.1111/lam.12285

Andrade, A., Paradis, A.-L., Rouquette, S., Poline, J.-B., 1999. Ambiguous Results in Functional Neuroimaging Data Analysis Due to Covariate Correlation. Neuroimage 10, 483–486. https://doi.org/10.1006/nimg.1999.0479

Ardia, D., Boudt, K., Carl, P., Mullen, K.M., Peterson, B.G., 2011. Differential Evolution with DEoptim An Application to Non-Convex Portfolio Optimization. R J. 3, 27–34.

Astals, S., Venegas, C., Peces, M., Jofre, J., Lucena, F., Mata-Alvarez, J., 2012. Balancing hygienization and anaerobic digestion of raw sewage sludge. Water Res. 46, 6218–6227. https://doi.org/10.1016/j.watres.2012.07.035

Auer, M.T., Niehaus, S.L., 1993. Modeling fecal coliform bacteria-I. Field and laboratory determination of loss kinetics. Water Res. 27, 693–701. https://doi.org/10.1016/0043-1354(93)90179-L

Augustynczik, A.L.D., Hartig, F., Minunno, F., Kahle, H.P., Diaconu, D., Hanewinkel, M., Yousefpour, R., 2017. Productivity of Fagus sylvatica under climate change – A Bayesian analysis of risk and uncertainty using the model 3-PG. For. Ecol. Manage. 401, 192–206. https://doi.org/10.1016/j.foreco.2017.06.061

Auld, H., MacIver, D., Klaassen, J., 2004. Heavy rainfall and waterborne disease outbreaks: The Walkerton example. J. Toxicol. Environ. Heal. - Part A 67, 1879–1887. https://doi.org/10.1080/15287390490493475

Ballesté, E., Blanch, A.R., 2010. Persistence of Bacteroides species populations in a river as measured by molecular and culture techniques. Appl. Environ. Microbiol. 76, 7608–7616. https://doi.org/10.1128/AEM.00883-10

Ballesté, E., García-Aljaro, C., Blanch, A.R., 2018. Assessment of the Decay Rates of Microbial Source Tracking Molecular Markers and Fecal Indicator Bacteria from Different Sources. J. Appl. Microbiol. https://doi.org/10.1111/jam.14058

Beveridge, O.S., Humphries, S., Petchey, O.L., Beveridge, O., Humphries, S., Petchey, O.L., 2018. The interacting effects of temperature and fo length on trophic abundance and ecosystem f. J. Anim. Ecol. 79, 693–700.

Bonada, N., Resh, V.H., 2013. Mediterranean-climate streams and rivers: Geographically separated but ecologically comparable freshwater systems. Hydrobiologia 719, 1–29. https://doi.org/10.1007/s10750-013-1634-2

Bonjoch, X., Lucena, F., Blanch, A.R., 2009. The persistence of bifidobacteria populations in a river measured by molecular and culture techniques. J. Appl. Microbiol. 107, 1178–1185. https://doi.org/10.1111/j.1365-2672.2009.04297.x

Burkhardt, W., Calci, K.R., Watkins, W.D., Rippey, S.R., Chirtel, S.J., 2000. Inactivation of indicator microorganisms in estuarine waters. Water Res. 34, 2207–2214. https://doi.org/10.1016/S0043-1354(99)00399-1

Capello, M., Cutroneo, L., Ferretti, G., Gallino, S., Canepa, G., 2016. Changes in the physical characteristics of the water column at the mouth of a torrent during an extreme rainfall event. J. Hydrol. 541, 146–157. https://doi.org/10.1016/j.jhydrol.2015.12.009

Chick, H., 1908. An investigation of the laws of disinfection 92–158.

Cho, K.H., Pachepsky, Y.A., Oliver, D.M., Muirhead, R.W., Park, Y., Quilliam, R.S., Shelton, D.R., 2016. Modeling fate and transport of fecally-derived microorganisms at the watershed scale: State of the science and future opportunities. Water Res. 100, 38–56. https://doi.org/10.1016/j.watres.2016.04.064

Cook, B.I., Smerdon, J.E., Seager, R., Coats, S., 2014. Global warming and 21st century drying. Clim. Dyn. 43, 2607–2627. https://doi.org/10.1007/s00382-014-2075-y

Curriero, F.C., Patz, J.A., Rose, J.B., Lele, S., 2001. The association between extreme precipitation and waterborne disease outbreaks in the United States, 1948-1994. Am. J. Public Health 91, 1194–1199. https://doi.org/10.2105/AJPH.91.8.1194

Dankovich, T.A., Levine, J.S., Potgieter, N., Dillingham, R., Smith, J.A., 2016. Inactivation of bacteria from contaminated streams in Limpopo, South Africa by silver- or copper-nanoparticle paper filters. Environ. Sci. Water Res. Technol. 2, 85–96. https://doi.org/10.1039/c5ew00188a

Davies, C.M., Long, J.A.H., Donald, M., Ashbolt, N.J., 1995. Survival of Fecal Microorganisms in Marine and Freshwater Sediments. Appl. Environ. Microbiol. 61, 1888–1896.

Fauvel, B., Gantzer, C., Cauchie, H.M., Ogorzaly, L., 2017. In Situ Dynamics of F-Specific RNA Bacteriophages in a Small River: New Way to Assess Viral Propagation in Water Quality Studies. Food Environ. Virol. 9, 89–102. https://doi.org/10.1007/s12560-016-9266-0

Fiorentino, A., De Luca, G., Rizzo, L., Viccione, G., Lofrano, G., Carotenuto, M., 2018. Simulating the fate of indigenous antibiotic resistant bacteria in a mild slope wastewater polluted stream. J. Environ. Sci. 69, 95–104. https://doi.org/10.1016/j.jes.2017.04.018

Galfi, H., Österlund, H., Marsalek, J., Viklander, M., 2016. Indicator bacteria and associated water quality constituents in stormwater and snowmelt from four urban catchments. J. Hydrol. 539, 125–140. https://doi.org/10.1016/j.jhydrol.2016.05.006

García-Aljaro, C., Blanch, A.R., Campos, C., Jofre, J., Lucena, F., 2018. Pathogens, faecal indicators and human-specific microbial source-tracking markers in sewage, Journal of Applied Microbiology. https://doi.org/10.1111/jam.14112

García-Aljaro, C., Martín-Díaz, J., Viñas-Balada, E., Calero-Cáeres, W., Lucena, F., Blanch, A.R., 2017. Mobilisation of microbial indicators, microbial source tracking markers and pathogens after rainfall events. Water Res. 112, 248–253. https://doi.org/10.1016/j.watres.2017.02.003

Gómez-Doñate, M., Ballesté, E., Muniesa, M., Blanch, A.R., 2012. New molecular quantitative pcr assay for detection of host-specific bifidobacteriaceae suitable for microbial source tracking. Appl. Environ. Microbiol. 78, 5788–5795. https://doi.org/10.1128/AEM.00895-12

Gordon, N.D., Thomas, A., Finlayson, B.L., Wiley, J., 1992. Stream Hydrology: An introduction for Ecologists. Chinchester, England.

Gourmelon, M., Caprais, M.P., Ségura, R., Le Mennec, C., Lozach, S., Piriou, J.Y., Rincé, A., 2007. Evaluation of two library-independent microbial source tracking methods to identify sources of fecal contamination in French estuaries. Appl. Environ. Microbiol. 73, 4857–4866. https://doi.org/10.1128/AEM.03003-06

Hartig, F., Dislich, C., Wiegand, T., Huth, A., 2014. Technical Note : Approximate Bayesian parameterization of a process-based tropical forest model 1261–1272. https://doi.org/10.5194/bg-11-1261-2014

Hartig, F., Dyke, J., Hickler, T., Higgins, S.I., O'Hara, R.B., Scheiter, S., Huth, A., 2012. Connecting dynamic vegetation models to data - an inverse perspective. J. Biogeogr. 39, 2240–2252. https://doi.org/10.1111/j.1365-2699.2012.02745.x

Hassan, G.E., Youssef, M.E., Mohamed, Z.E., Ali, M.A., Hanafy, A.A., 2016. New Temperature-based Models for Predicting Global Solar Radiation. Appl. Energy 179, 437–450. https://doi.org/10.1016/j.apenergy.2016.07.006

IPCC, 2013. Climate Change 2013: The Physical Science Basis. Contribution of Working Group I to the Fifth Assessment Report of the Intergovern- mental Panel on Climate Change [Stocker, T.F., D. Qin, G.-K. Plattner, M. Tignor, S.K. Allen, J. Boschung, A. Nauels, Y. Xi, Climate Change 2013: The Physical Science Basis. Contribution of Working Group I to the Fifth Assessment Report of the Intergovernmental Panel on Climate Change.

Ishii, S., Sadowsky, M.J., 2008. Escherichia coli in the Environment: Implications for Water Quality and Human Health. Microbes Environ. 23, 101–108. https://doi.org/10.1264/jsme2.23.101

ISO, 2001. International Standard ISO 10705-4: Water Quality - Detection and Enumeration of Bacteriophages. Part 4: Enumeration of bacteriophages infect- ing Bacteroides fragilis.

ISO, 2000. International Standard ISO 10705-2: Water Quality - Detection and Enumeration of Bacteriophages. Part 2: Enumeration of somatic coliphages.

Jamieson, R., Joy, D.M., Lee, H., Kostaschuk, R., Gordon, R., 2005. Transport and deposition of sediment-associated Escherichia coli in natural streams. Water Res. 39, 2665–2675. https://doi.org/https://doi.org/10.1016/j.watres.2005.04.040

Jofre, J., Blanch, A.R., Lucena, F., Muniesa, M., 2014. Bacteriophages infecting Bacteroides as a marker for microbial source tracking. Water Res. 55, 1–11. https://doi.org/10.1016/j.watres.2014.02.006

Jonsson, A., Agerberg, S., 2015. Modelling of E. coli transport in an oligotrophic river in northern Scandinavia. Ecol. Modell. 306, 145–151. https://doi.org/10.1016/j.ecolmodel.2014.10.021

Lagarrigues, G., Jabot, F., Lafond, V., Courbaud, B., 2015. Approximate Bayesian computation to recalibrate individual-based models with population data : Illustration with a forest simulation model. Ecol. Modell. 306, 278–286. https://doi.org/10.1016/j.ecolmodel.2014.09.023

Li, H., Cao, F., Wang, X., Ma, W., 2014. A Temperature-Based Model for Estimating Monthly Average Daily Global Solar Radiation in China. Sci. World J. 2014.

Lionello, P., Abrantes, F., Gacic, M., Planton, S., Trigo, R., Ulbrich, U., 2014. The climate of the Mediterranean region: research progress and climate change impacts. Reg. Environ. Chang. 14, 1679–1684. https://doi.org/10.1007/s10113-014-0666-0

Lionello, P., Malanotte-Rizzoli, P., Boscolo, R., Alpert, P., Artale, V., Li, L., Luterbacher, J., May, W., Trigo, R., Tsimplis, M., Ulbrich, U., Xoplaki, E., 2006. The Mediterranean Climate: An Overview of the Main Characteristics and Issues. Dev. Earth Environ. Sci. 4, 1–26.

Lionello, P., Scarascia, L., 2018. The relation between climate change in the Mediterranean region and global warming. Reg. Environ. Chang. 18, 1481–1493. https://doi.org/10.1007/s10113-018-1290-1

Mariotti, A., Pan, Y., Zeng, N., Alessandri, A., 2015. Long-term climate change in the

Mediterranean region in the midst of decadal variability. Clim. Dyn. 44, 1437–1456. https://doi.org/10.1007/s00382-015-2487-3

Martín-Díaz, J., García-Aljaro, C., Pascual-Benito, M., Galofré, B., Blanch, A.R., Lucena, F., 2017. Microcosms for evaluating microbial indicator persistence and mobilization in fluvial sediments during rainfall events. Water Res. 123, 623–631. https://doi.org/10.1016/j.watres.2017.07.017

Merseburger, G.C., Martí, E., Sabater, F., 2005. Net changes in nutrient concentrations below a point source input in two streams draining catchments with contrasting land uses. Sci. Total Environ. 347, 217–229. https://doi.org/10.1016/j.scitotenv.2004.12.022

Milano, M., Ruelland, D., Fernandez, S., Dezetter, A., Fabre, J., Servat, E., Fritsch, J.M., Ardoin-Bardin, S., Thivet, G., 2013. Current state of Mediterranean water resources and future trends under climatic and anthropogenic changes. Hydrol. Sci. J. 58, 498–518. https://doi.org/10.1080/02626667.2013.774458

Morrill, J.C., Bales, R.C., M.ASCE, Conklin, M.H., 2005. Estimating stream temperature from Air temperature: Implications for future water quality. J. Environ. Eng. 131, 139–146. https://doi.org/10.1061/(asce)0733-9372(2005)131:1(139)

Mosley, L.M., 2015. Drought impacts on the water quality of freshwater systems; review and integration. Earth-Science Rev. 140, 203–214. https://doi.org/10.1016/j.earscirev.2014.11.010

Muirhead, R.W., Davies-Colley, R.J., Donnison, A.M., Nagels, J.W., 2004. Faecal bacteria yields in artificial flood events: Quantifying in-stream stores. Water Res. 38, 1215–1224. https://doi.org/10.1016/j.watres.2003.12.010

Mullen, K.M., Ardia, D., Gil, D.L., Cline, J., 2011. DEoptim : An R Package for Global Optimization by Differential Evolution 40.

Muniesa, M., Lucena, F., Blanch, A.R., Payán, A., Jofre, J., 2012. Use of abundance ratios of somatic coliphages and bacteriophages of Bacteroides thetaiotaomicron GA17 for microbial source identification. Water Res. 46, 6410–6418. https://doi.org/10.1016/j.watres.2012.09.015

Muñoz, I., López-Doval, J.C., Ricart, M., Villagrasa, M., Brix, R., Geiszinger, A., Ginebreda, A., Guasch, H., López de Alda, M.J., Romaní, A.M., Sabater, S., Barceló, D., 2009. Bridging levels of pharmaceuticals in river water with biological community structure in the Llobregat river basin (northeast Spain). Environ. Toxicol. Chem. 28, 2706–2714.

Nguyen, K.H., Senay, C., Young, S., Nayak, B., Lobos, A., Conrad, J., Harwood, V.J., 2018. Determination of wild animal sources of fecal indicator bacteria by microbial source tracking (MST) influences regulatory decisions. Water Res. 144, 424–434. https://doi.org/10.1016/j.watres.2018.07.034

O'Hara, R.B., Arjas, E., Toivonen, H., Hanski, I., 2002. Bayesian analysis of metapopulation data. Ecology 83, 2408–2415. https://doi.org/10.1890/0012-9658(2002)083[2408:BAOMD]2.0.CO;2

Orlowsky, B., Seneviratne, S.I., 2013. Elusive drought: Uncertainty in observed trends and short-and long-term CMIP5 projections. Hydrol. Earth Syst. Sci. 17, 1765–1781. https://doi.org/10.5194/hess-17-1765-2013

Otero, I., Boada, M., Badia, A., Pla, E., Vayreda, J., Sabaté, S., Gracia, C.A., Peñuelas, J., 2011. Loss of water availability and stream biodiversity under land abandonment and climate change in a Mediterranean catchment (Olzinelles, NE Spain). Land use policy 28, 207–218. https://doi.org/10.1016/j.landusepol.2010.06.002

Pascual-Benito, M., García-Aljaro, C., Casanovas-Massana, S., Blanch, A.R., Lucena, F., 2015. Effect of hygienization treatment on the recovery and/or regrowth of microbial indicators in sewage sludge. J. Appl. Microbiol. 118, 412–418. https://doi.org/10.1111/jam.12708

Pilgrim, J.M., Fang, X., Stefan, H.G., 1998. Stream temperature correlations with air temperatures in Minnesota: Implications for climate warming. J. Am. Water Resour. Assoc. 34, 1109–1121. https://doi.org/10.1111/j.1752-1688.1998.tb04158.x

Prieto, J.I., Martínez-García, J.C., García, D., 2009. Correlation between global solar irradiation and air temperature in Asturias , Spain. Sol. Energy 83, 1076–1085. https://doi.org/10.1016/j.solener.2009.01.012

Purves, D.W., Zavala, M.A., Ogle, K., Prieto, F., Rey Benayas, J.M., 2007. Environmental heterogeneity, bird-mediated directed dispersal, and oak woodland dynamics in Mediterranean Spain. Ecol. Monogr. 77, 77–97. https://doi.org/10.1890/05-1923

Romo, S., Soria, J., Fernández, F., Ouahid, Y., Barón-Solá, Á., 2013. Water residence time and the dynamics of toxic cyanobacteria. Freshw. Biol. 58, 513–522. https://doi.org/10.1111/j.1365-2427.2012.02734.x

Rose, J.B., Epstein, P.R., Lipp, E.K., Sherman, B.H., M, S., Patz, J.A., Environmental, S., Perspectives, H., May, S., Bernard, S.M., 2010. and Change in the United States : Potential Impacts on Water- Climate Variability and Foodborne Diseases Caused by Microbiologic Agents. Environ. Heal. 109, 211–220.

Ruiz-Hernando, M., Martín-Díaz, J., Labanda, J., Mata-Alvarez, J., Llorens, J., Lucena, F., Astals, S., 2014. Effect of ultrasound, low-temperature thermal and alkali pre-treatments on waste activated sludge rheology, hygienization and methane potential. Water Res. 61, 119–129. https://doi.org/10.1016/j.watres.2014.05.012

Runkel, R., 1998. OTIS - (One-Dimensional Transport with Inflow and Storage: A Solute Transport Model for Streams and Rivers). US Geol. Surv. https://doi.org/10.1002/0470848944.hsa266

Saxena, G., Bharagava, R.N., Kaithwas, G., Raj, A., 2015. Microbial indicators, pathogens and methods for their monitoring in water environment. J. Water Health 13, 319–339. https://doi.org/10.2166/wh.2014.275

Serrano-Notivoli, R., Martín-Vide, J., Saz, M.A., Longares, L.A., Beguería, S., Sarricolea, P., Meseguer-Ruiz, O., de Luis, M., 2018. Spatio-temporal variability of daily precipitation concentration in Spain based on a high-resolution gridded data set. Int. J. Climatol. 38, e518–e530. https://doi.org/10.1002/joc.5387

Sinton, L.W., Finlay, R.K., Lynch, P.A., 1999. Sunlight inactivation of fecal bacteriophages and bacteria in sewage- polluted seawater. Appl. Environ. Microbiol. 65, 3605–3613. https://doi.org/10.1373/clinchem.2008.112797

Sinton, L.W., Hall, C.H., Lynch, P.A., Davies-Colley, R.J., 2002. Sunlight inactivation of fecal indicator bacteria and bacteriophages from waste stabilization pond effluent in fresh and saline waters. Appl. Environ. Microbiol. 68, 1122–1131. https://doi.org/10.1128/AEM.68.3.1122-1131.2002

Stella, J.C., M, R.-G.P., S, D., Bendix, J., 2013. How are riparian plants distributed along the riverbank topographic gradient in Mediterranean rivers? Application to minimally altered river stretches in Southern Spain. Hydrobiologia 719, 291–315. https://doi.org/10.1007/s10750-012-1304-9

Super, M., Heese, H. de V., MacKenzie, D., Dempster, W.S., du Plessis, J., Ferreira, J.J., 1981. An epidemiological study of well-water nitrates in a group of south west african/namibian infants. Water Res. 15, 1265–1270. https://doi.org/10.1016/0043-1354(81)90103-2

Ter Braak, C.J.F., Vrugt, J.A., 2008. Differential Evolution Markov Chain with snooker updater and fewer chains. Stat. Comput. 18, 435–446. https://doi.org/10.1007/s11222-008-9104-9

Thivet, G., Blinda, M., 2011. Water for forests resources and people in the Mediterranean: the current situation in Woter for forest ans people in the Mediterranean region - A challenging balance, European Forest Institute.

Vinten, A.J.A., Lewis, D.R., McGechan, M., Duncan, A., Aitken, M., Hill, C., Crawford, C., 2004. Predicting the effect of livestock inputs of E. coli on microbiological compliance of bathing waters. Water Res. 38, 3215–3224. https://doi.org/10.1016/j.watres.2004.04.033

WHO, 2017. Guidance for producing safe drinking-water.

WHO, 2009. Water Safety Plan Manual: Step-by-step risk management for drinking-water suppliers 108. https://doi.org/10.1111/j.1752-1688.1970.tb00528.x

WHO, 2001. Guidelines , Standards and Health : Assessment of risk and risk management for water-related infectious disease 1–431.

Wu, J., Cao, Y., Young, B., Yuen, Y., Jiang, S., Melendez, D., Griffith, J.F., Stewart, J.R., 2016. Decay of Coliphages in Sewage-Contaminated Freshwater: Uncertainty and Seasonal Effects. Environ. Sci. Technol. 50, 11593–11601. https://doi.org/10.1021/acs.est.6b03916

Yakirevich, A., Pachepsky, Y.A., Guber, A.K., Gish, T.J., Shelton, D.R., Cho, K.H., 2013. Modeling transport of Escherichia coli in a creek during and after artificial high-flow events: Three-year study and analysis. Water Res. 47, 2676–2688. https://doi.org/10.1016/j.watres.2013.02.011

Zhao, P., Yu, B., 2006. On Model Selection Consistency of Lasso. J. Mach. Learn. Res. 7, 2541–2563.

Table 1. Mean concentrations and standard deviation of faecal indicator organisms (FIO) before and after the wastewater treatment plant (WWTP) for the wet (n=7) and dry season (n=3). Data is given in $\log_{10}$ CFU per 100 ml for *E. coli* and spores of sulphite-reducing clostridia (SSRC), in $\log_{10}$ PFU per 100 ml for SOMCPH and GA17PH and $\log_{10}$ GC per 100 ml for HMBif. Statistically significant differences after a t-test between Before (upstream of the WWTP) and After (75 m downstream of the WWTP) concentrations for each season (bold font) and between After concentrations during wet and dry seasons (font) are also noted ($p<0.05$, n (Wet season) =7, n (Dry season) = 3).

E. coli; SSRC: spores of sulphite-reducing clostridia; SOMCPH: somatic coliphages; GA17PH: GA17 bacteriophages; HMBif: human-specific *Bifidobacterium* molecular marker.

	Wet season concentration		Dry season concentration	
Indicator	Before WWTP	After WWTP	Before WWTP	After WWTP
E. coli	**2.64±0.5**	**4.25±0.5**	**3.46±0.0**	**4.21±0.3**
SSRC	**2.23±0.4**	**3.36±0.4**	**2.22±0.9**	**3.42±0.2**
SOMCPH	**1.80±0.7**	**3.93±0.2**	**1.75±0.4**	**4.21±0.1**
GA17PH	**0.17±0.3**	**1.29±0.6**	**0.79±1.1**	**1.83±0.4**
HMBif	**3.60±0.8**	**5.52±0.6**	**3.67±0.0**	**4.19±1.4**

Table 2. Mean decay rates (k, in km^{-1}) and self-depuration distances (SDD, in km) with the standard deviation for the five faecal indicator organisms (FIO). Decay rate (unit less) is given in $k \cdot 10^{-3}$, while SDD is given in km. Statistically significant differences after a t-test between Dry and Wet seasons are noted in bold font ($p<0.05$, n (Wet) =7, n (Dry) = 3)**.**

E. coli; SSRC: spores of sulphite-reducing clostridia; SOMCPH: somatic coliphages; GA17PH: GA17 bacteriophages; HMBif: human-specific *Bifidobacterium* molecular marker.

	k (km^{-1})		SDD (km)	
Indicator	Dry season	Wet season	Dry season	Wet season
E. coli	-3.6±2.0	-1.2±0.5	**0.6±0.4**	**3.1±0.7**
SSRC	-1.2±0.0	-0.8±0.4	2.1±1.8	4.4±3.8
SOMCPH	**-1.6±0.5**	**-0.9±0.4**	4.0±0.5	5.5±1.6
GA17PH	-2.5±1.0	-0.7±0.5	2.7±1.9	4.3±3.4
HMBif	-1.8±0.0	-1.2±0.8	2.0±0.0	5.0±3.5

Figure 1. Evolution of: a) precipitation (light blue) and cumulative precipitation (dark blue), in mm; b) Q_{stream} (blue line), $Q_{effluent}$ (red line) and $Q_{downstream}$ (green line) in $10^{-3} \cdot m^3 \cdot s^{-1}$; c) maximum (red line) and minimum temperature (blue line), in °C and d) contribution of the Q_{stream} to the $Q_{downstream}$ (dilution factor) during 2016-2017.

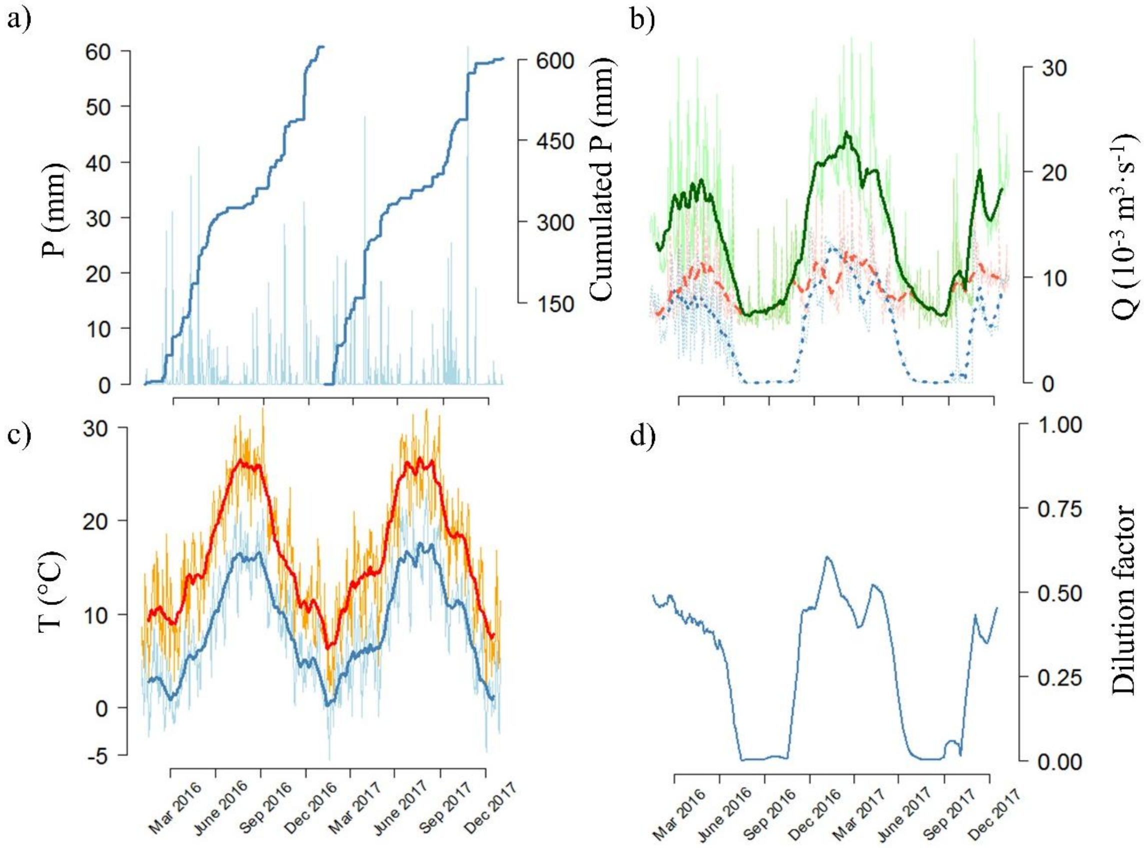

Figure 2. Agreement between observed and modelled *k* values for all sampling campaigns and each faecal indicator organism (FIO). Regression (dashed line) compared to 1:1 (solid line), RMSE and R^2 are noted for each FIO.

The intercept was always not statistically different from zero after a Student t-test. RMSE measures the error for each individual k estimate. R^2 is the variability within the data explained by the model. All modes were visually checked for homoskedasticity and normality of their residuals.

E. coli; SSRC: spores of sulphite-reducing clostridia; SOMCPH: somatic coliphages; GA17PH: GA17 bacteriophages; HMBif: human-specific *Bifidobacterium* molecular marker.

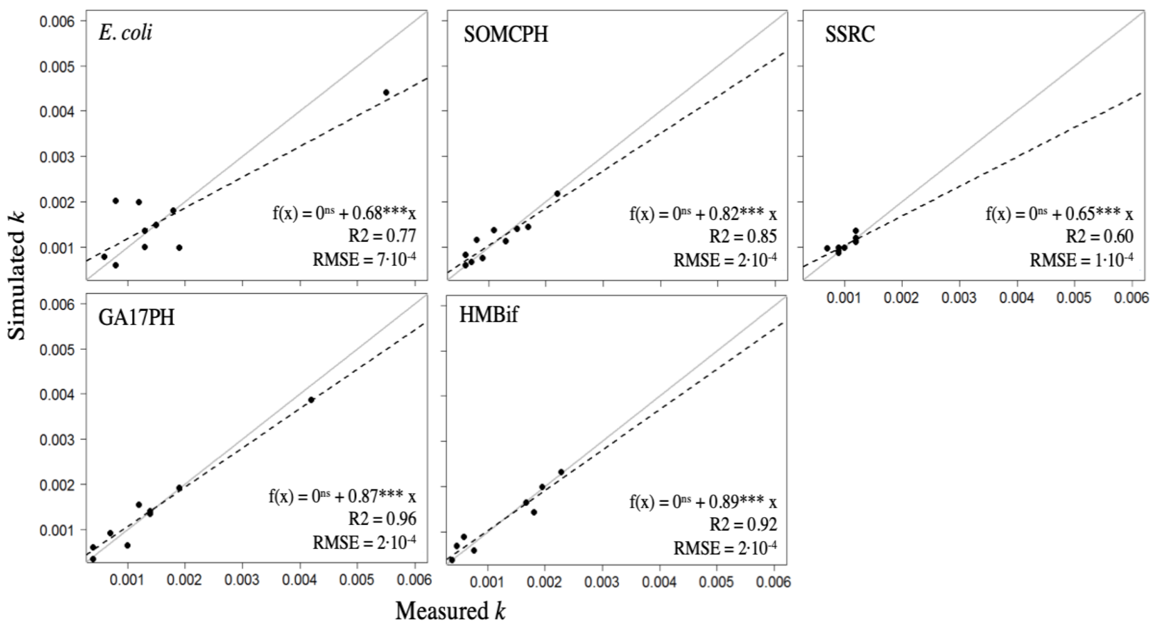

Figure 3. Response of faecal indicator organisms (FIO) to streamflow and temperature according to equations 5 and 6.

E. coli (solid blue line); SSRC: spores of sulphite-reducing clostridia (dashed blue line); SOMCPH: somatic coliphages (solid red line); GA17PH: GA17 bacteriophages (dashed red line); HMBif: human-specific *Bifidobacterium* marker (dotted red line).

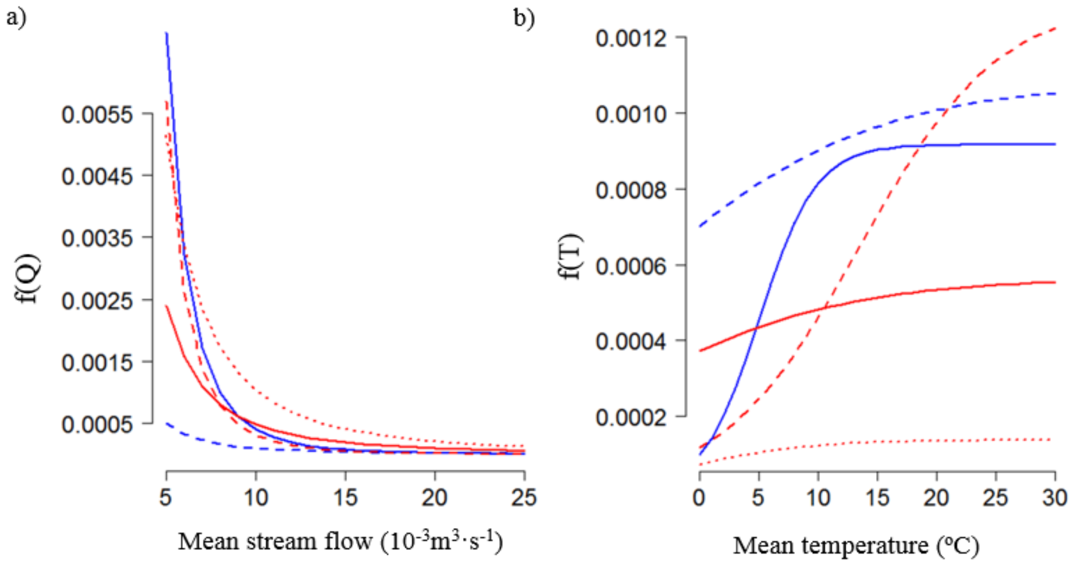

Figure 4. Monthly median contribution of temperature (T) to the total decay rate (*k*).

E. coli; SSRC: spores of sulphite-reducing clostridia; SOMCPH: somatic coliphages; GA17PH: GA17 bacteriophages; HMBif: human-specific *Bifidobacterium* molecular marker.

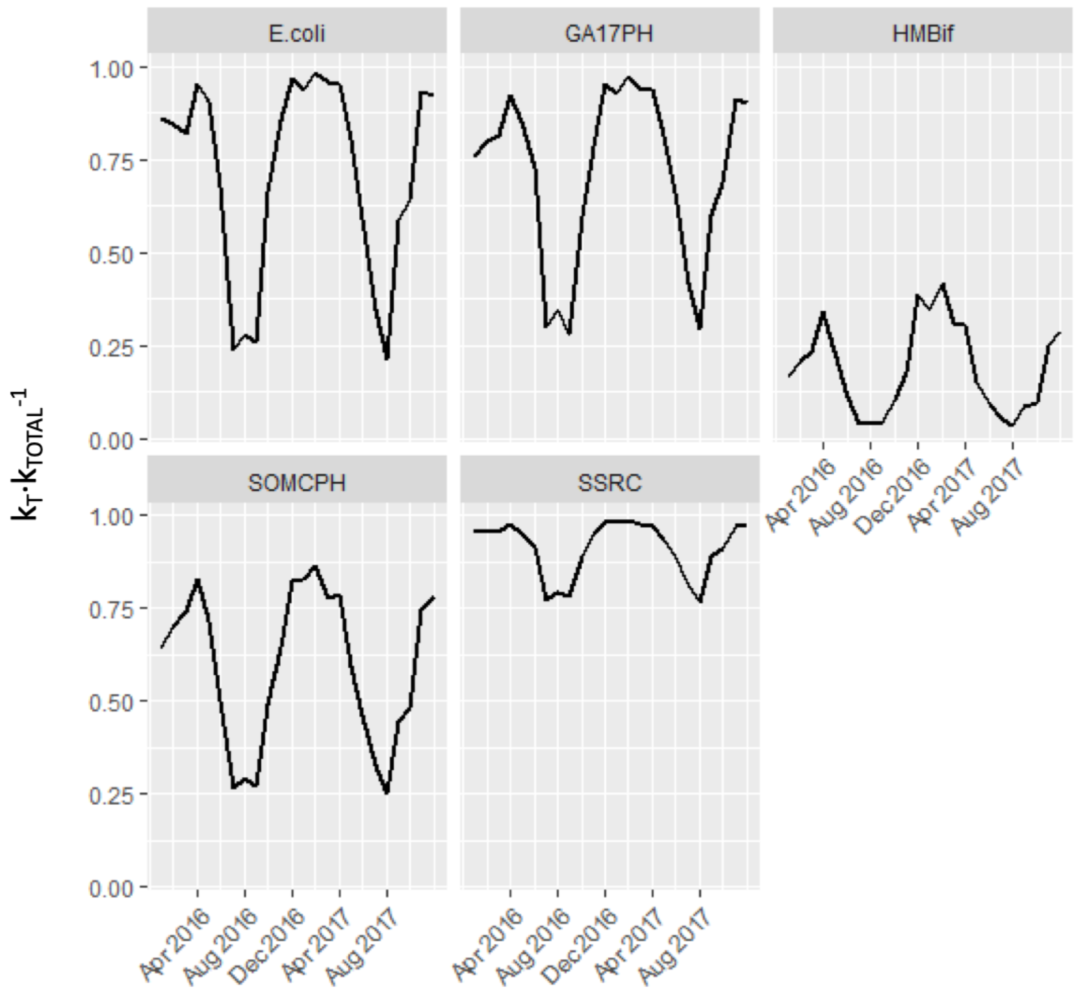

Figure 5. Modelled decay rate (k, in m^{-1}) for the studied faecal indicator organisms.

E. coli; SSRC: spores of sulphite-reducing clostridia; SOMCPH: somatic coliphages; GA17PH: GA17 bacteriophages; HMBif: human-specific *Bifidobacterium* molecular marker.

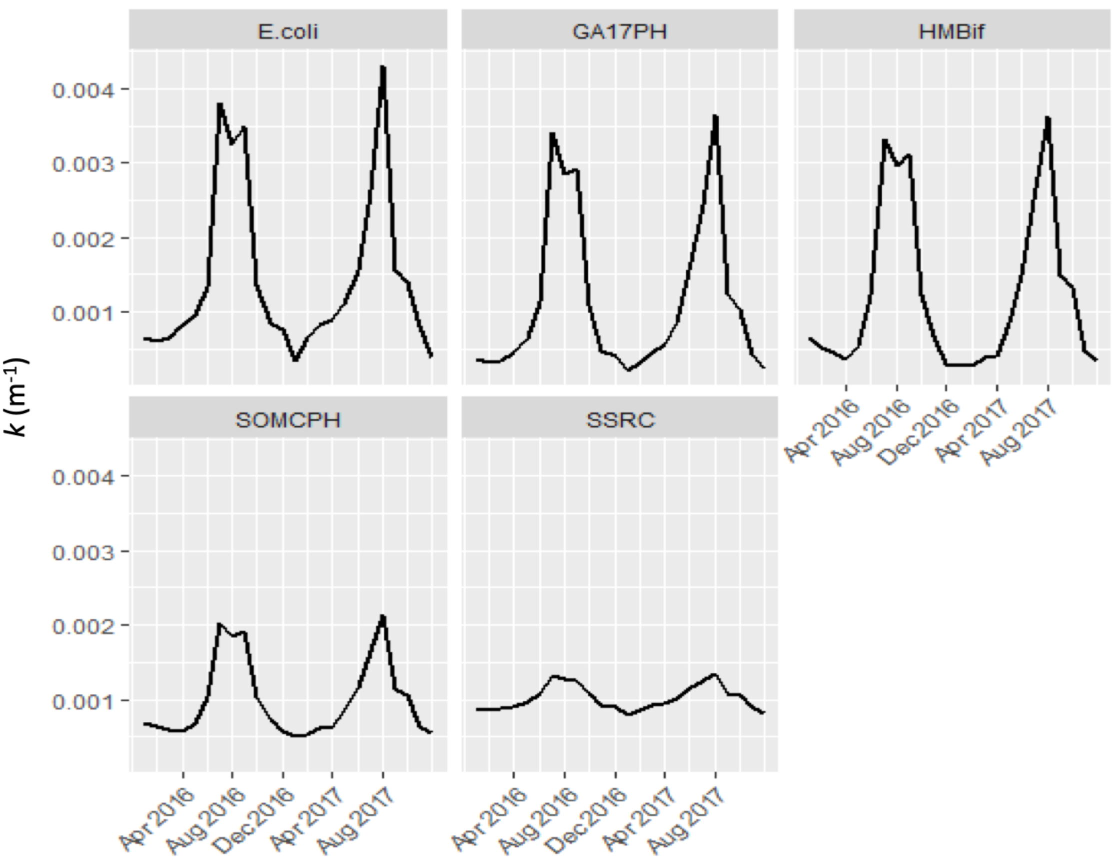

Figure 6. Modelled self-depuration distance (SDD) for the studied faecal indicator organisms.

E. coli; SSRC: spores of sulphite-reducing clostridia; SOMCPH: somatic coliphages; GA17PH: GA17 bacteriophages; HMBif: human-specific *Bifidobacterium* molecular marker.

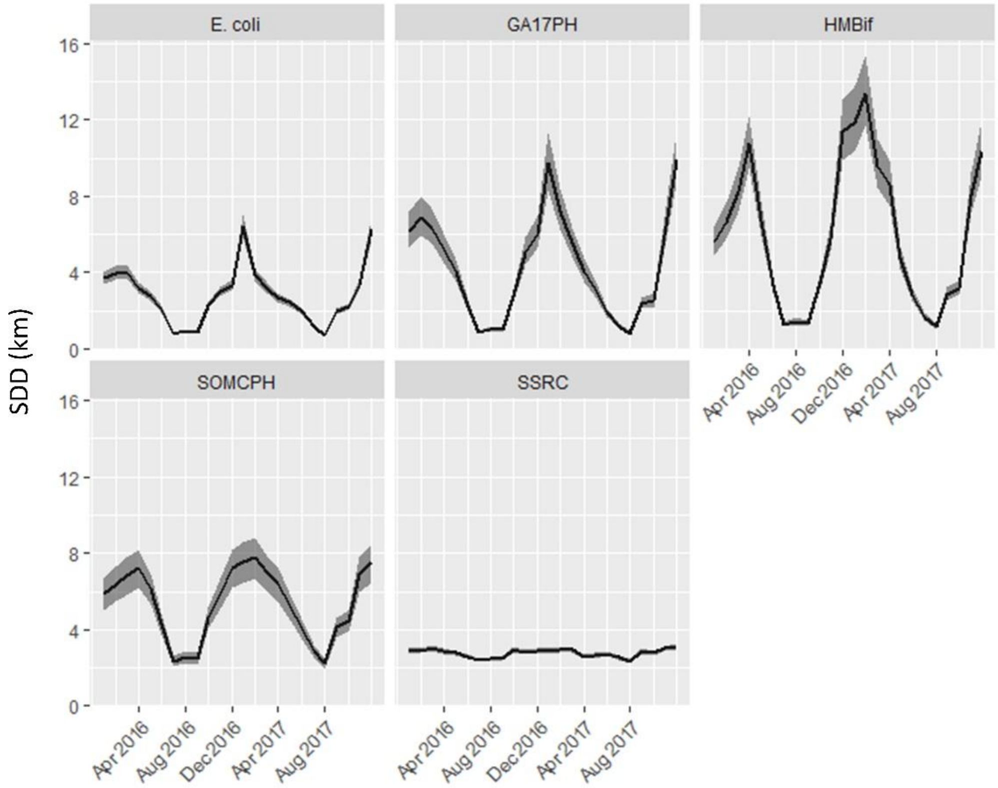

Supplementary Material 1. Coefficients to calculate the dependences on streamflow (Q) and temperature (T) according to equations 5 and 6, and R^2 and RMSE between observed and simulated *k*.

E. coli; SSRC: spores of sulphite-reducing clostridia; SOMCPH: somatic coliphages; GA17PH: GA17 bacteriophages; HMBif: human-specific *Bifidobacterium* molecular marker.

	$f(Q_{downstream})$		$f(T_{air})$				
Indicator	*a*	*b*	*c*	*d*	*e*	R^2	RMSE
E. coli	4.91	-4.09	$1.1\cdot10^{-4}$	0.42	0.12	0.77	$7\cdot10^{-4}$
SOMCPH	0.097	-2.3	$1.1\cdot10^{-3}$	0.11	1.95	0.84	$2\cdot10^{-4}$
SSRC	0.024	-2.4	$2\cdot10^{-3}$	0.1	1.85	0.6	$1\cdot10^{-4}$
GA17PH	4.99	-4.21	$1.3\cdot10^{-4}$	0.17	0.1	0.96	$2\cdot10^{-4}$
HMBif	0.212	-2.31	$1.6\cdot10^{-4}$	0.2	1.16	0.92	$2\cdot10^{-4}$

***Credit Author Statement**

AUTHOR DECLARATION TEMPLATE

We confirm that the manuscript has been read and approved by all named authors and that there are no other persons who satisfied the criteria for authorship but are not listed. We further confirm that the order of authors listed in the manuscript has been approved by all of us.

We confirm that we have given due consideration to the protection of intellectual property associated with this work and that there are no impediments to publication, including the timing of publication, with respect to intellectual property. In so doing we confirm that we have followed the regulations of our institutions concerning intellectual property.

We understand that the Corresponding Author is the sole contact for the Editorial process (including Editorial Manager and direct communications with the office). She is responsible for communicating with the other authors about progress, submissions of revisions and final approval of proofs. We confirm that we have provided a current, correct email address which is accessible by the Corresponding Author and which has been configured to accept email from mpascualbenito@ub.edu.

Signed by all authors as follows:

Miriam Pascual-Benito

Daniel Nadal-Sala

Marta Tobella

Elisenda Ballesté

Cristina García-Aljaro

Santiago Sabaté

Francesc Sabater

Eugènia Martí

Carlos A. Gracia

Anicet R. Blanch

Francisco Lucena

DECLARATION OF INTEREST STATEMENT

We wish to confirm that there are no known conflicts of interest associated with this publication and there has been no significant financial support for this work that could have influenced its outcome.

Signed by all authors as follows:

Miriam Pascual-Benito

Daniel Nadal-Sala

Marta Tobella

Elisenda Ballesté

Cristina García-Aljaro

Santiago Sabaté

Francesc Sabater

Eugènia Martí

Carlos A. Gracia

Anicet R. Blanch

Francisco Lucena